Cell-to-Cell Movement of Green Fluorescent Protein Reveals Post-Phloem Transport in the Outer Integument and Identifies Symplastic Domains in Arabidopsis Seeds and Embryos[1]

Ruth Stadler, Christian Lauterbach[2], and Norbert Sauer*

Molekulare Pflanzenphysiologie, Universität Erlangen-Nürnberg, D–91058 Erlangen, Germany

Developing Arabidopsis (*Arabidopsis thaliana*) seeds and embryos represent a complex set of cell layers and tissues that mediate the transport and partitioning of carbohydrates, amino acids, hormones, and signaling molecules from the terminal end of the funicular phloem to and between these seed tissues and eventually to the growing embryo. This article provides a detailed analysis of the symplastic domains and the cell-to-cell connectivity from the end of the funiculus to the embryo, and within the embryo during its maturation. The cell-to-cell movement of the green fluorescent protein or of mobile and nonmobile green fluorescent protein fusions was monitored in seeds and embryos of plants expressing the corresponding cDNAs under the control of various promoters (*SUC2*, *SUC3*, *TT12*, and *GL2*) shown to be active in defined seed or embryo cell layers (*SUC3*, *TT12*, and *GL2*) or only outside the developing Arabidopsis seed (*AtSUC2*). Cell-to-cell movement was also analyzed with the low-molecular-weight fluorescent dye 8-hydroxypyrene-1,3,6-trisulfonate. The analyses presented identify a phloem-unloading domain at the end of the funicular phloem, characterize the entire outer integument as a symplastic extension of the phloem, and describe the inner integument and the globular stage embryo plus the suspensor as symplastic domains. The results also show that, at the time of hypophysis specification, the symplastic connectivity between suspensor and embryo is reduced or interrupted and that the embryo develops from a single symplast (globular and heart stage) to a mature embryo with new symplastic domains.

Long-distance allocation and partitioning of photoassimilates in higher plants is mediated via highly specialized cells in the phloem. In Arabidopsis (*Arabidopsis thaliana*), Suc is loaded into the companion cells (CCs) of fully developed source leaves and moves symplastically into the enucleate sieve elements (SEs). Sucrose loading into the CCs is catalyzed by the AtSUC2 Suc transporter (Stadler and Sauer, 1996), an energy-dependent H^+-symport protein (Sauer and Stolz, 1994) essential for Arabidopsis development (Gottwald et al., 2000). In contrast, other Suc transporters that were also identified in the vascular tissue (AtSUC3 [Meyer et al., 2000] and AtSUC4 [Weise et al., 2000]) do not seem to be essential for phloem transport. In Arabidopsis, small amounts of the loaded Suc are converted into raffinose (Haritatos et al., 2000), which is a major component of the phloem sap in other plant species. Driven by Münch's mass flow, both compounds are allocated to the different sink organs.

In contrast to this quite clear situation on the loading side of the Arabidopsis phloem (one organ [the source leaves], one mechanism [apoplastic loading], and mainly one protein for the loading of carbohydrates [AtSUC2]), the situation is much more complex at its unloading ends. Developmental status and environmental conditions (Sun et al., 2004) influence and alter the type, number, and size of the competing sink organs. Several groups have provided evidence that unloading at the terminal ends of the phloem is mostly symplastic through plasmodesmata (Fisher and Oparka, 1996; Patrick, 1997; Hoth et al., 2005; Stadler et al., 2005), but apoplastic phloem unloading has also been reported (Zhang et al., 2004).

Imlau et al. (1999) and Oparka et al. (1999) introduced green fluorescent protein (GFP) as a versatile symplastic probe that is reasonably stable in plant cells and that moves cell to cell both after expression of its open reading frame (ORF) under the control of the CC-specific *AtSUC2* promoter (Imlau et al., 1999) or after microinjection of the GFP protein (Oparka et al., 1999). Only recently, Stadler et al. (2005) extended this approach and analyzed Arabidopsis plants expressing under the control of the *AtSUC2* promoter the ORFs for mobile and nonmobile GFP variants. In these proteins, GFP was fused to globular proteins of different molecular masses, membrane anchors, or targeting and retention signals for the endoplasmic reticulum. The authors were able to show that plasmodesmata in the SEs of the protophloem in Arabidopsis root tips have a large size exclusion limit (SEL; at least 67 kD) and allow the release of macromolecules into a newly

[1] This work was supported by the Deutsche Forschungsgemeinschaft (grant nos. SA 382/8 and SA 382/12 to N.S.).

[2] Present address: Scottish Crop Research Institute, Invergowrie, Dundee DD2 5DA, UK.

* Corresponding author; e-mail nsauer@biologie.uni-erlangen.de; fax 49–9131–8528751.

Article, publication date, and citation information can be found at www.plantphysiol.org/cgi/doi/10.1104/pp.105.065607.

described unloading domain. However, only GFP (27 kD) was able to exit this unloading domain and move symplastically into other cells of the Arabidopsis root tip, whereas larger GFP fusions (36 to 67 kD) were held back or trapped inside this unloading domain (Stadler et al., 2005). Meyer et al. (2004) showed that post-phloem movement of GFP within the root tip is not directed and that GFP synthesized exclusively in the root-tip rhizodermis can move toward the central cylinder, suggesting that cell-to-cell movement in post-phloem sinks occurs by diffusion. In a similar approach, Hoth et al. (2005) used *AtSUC2* promoter/*GFP* plants for the analysis of plasmodesmata in syncytia, which represent secondary sinks that are formed in Arabidopsis roots upon infection with the cyst nematode *Heterodera schachtii*. Hoth and coworkers (2005) showed that these syncytia become symplastically connected to a newly formed phloem, mainly to the phloem SEs, and that CC-derived GFP can move into these SEs and eventually into the syncytia.

The most important sinks of each plant are its seeds. The maternal layers of angiosperm seeds, the seed coat or testa, nourish the developing filial organs (i.e. the endosperm and the embryo), protect the mature embryo, and eventually supply energy and organic carbon during germination. For the latter task, seeds form storage compartments and are therefore of major economic interest. For this reason, phloem unloading and post-phloem transport have been studied extensively in the caryopses of wheat (*Triticum aestivum*; Wang et al., 1994; Wang and Fisher, 1994; Fisher and Cash-Clark, 2000a, 2000b) and rice (*Oryza sativa*; Oparka and Gates, 1981; Krishnan and Dayanandan, 2003) or in grain legumes (Offler and Patrick, 1984, 1993; Weber et al., 1997a, 1997b; Tegeder et al., 1999; Patrick and Offler, 2001).

The testae of these plants have a vascular compartment embedded in their ground tissue. The sieve elements of this vascular compartment are symplastically connected to the ground tissue, which serves as a symplastic compartment that delivers the nutrients to the underlying filial tissues (Patrick and Offler, 2001). Several groups showed that the plasmodesmata involved in phloem unloading and post-phloem movement between the cells of the ground tissue have large SELs, which may account for the high permeabilities observed (Offler and Patrick, 1984; Murray, 1987; Wang and Fisher, 1994; Patrick and Offler, 1995; Patrick et al., 1995; Fisher and Cash-Clark, 2000a). The surprising result of one of these analyses (Fisher and Cash-Clark, 2000a) was that fluorescent tracers of up to 400 kD (fluorescein-labeled Ficoll with a Stokes radius [R_S] of about 11 nm) were unloaded from the wheat grain vascular bundle.

The seed anatomy in Arabidopsis differs strongly from that described for cereals and legumes. There is no vascular tissue within the developing Arabidopsis seed, a nucellar projection is not formed, and most of the nucellar cells have degenerated in the fully developed seed. The unique vascular bundle that translocates photoassimilates to an Arabidopsis seed terminates at the end of the funiculus and releases its content into the testa proximal to the micropyle, where the abscission zone (the hilum) will be formed in the mature seed (Robinson-Beers et al., 1992).

In this article, we dissect the potential symplastic/apoplastic pathway of photoassimilates in Arabidopsis seeds. We apply the noninvasive approach with transgenic plants expressing different phloem mobile or nonmobile GFPs under the control of different promoters (*AtSUC2*, *AtSUC3*, *AtTT12*, and *AtGL2*). Analyses of GFP cell-to-cell movement reveal the symplastic connectivity within and between the individual structures of the Arabidopsis seed (inner and outer integument, endosperm, suspensor, and embryo at different developmental stages). These analyses were supplemented by an invasive approach using the membrane-impermeable fluorescent dye 8-hydroxypyrene-1,3,6-trisulfonate (HPTS) and are compared to the expression patterns of different Suc transporter genes (AtSUC3 and AtSUC5) within the seed and the developing embryo.

The data presented identify the likely post-phloem path of photoassimilates released from the funicular end of the phloem to the developing Arabidopsis embryo. Our results demonstrate that the outer integument allows movement of unloaded photoassimilates and macromolecules and represents a symplastic extension of the funicular phloem. Furthermore, our analyses suggest that the supply of photoassimilates to the young, globular embryo occurs symplastically via the suspensor. The results also show that the SEL of the plasmodesmata connecting the suspensor and embryo is reduced at the time of hypophysis specification. Finally, the data presented demonstrate that Arabidopsis embryos constitute a single symplastic domain during the globular and heart stages and that additional symplastic domains are formed during embryo maturation.

RESULTS

Cells of the Outer Integument Form a Symplastic Continuum and Are Connected by Plasmodesmata with a Dilated Aperture

The mature Arabidopsis ovule is anatropous (inverted; i.e. the micropyle is in close vicinity to the funicular attachment site) and bitegmic (i.e. it has two integument layers; Mansfield and Bowman, 1993). Imlau et al. (1999) had shown that, in *AtSUC2* promoter/*GFP* plants, GFP moved from the CCs into the SEs and was translocated into the testa of developing seeds.

A more detailed analysis of the post-phloem transport of GFP within the testa of these plants by confocal laser-scanning microscopy (CLSM) revealed that movement of unloaded GFP (Fig. 1A) does not occur in all cell layers of the testa. Rather, it is restricted to the two cell layers that form the outer integument of the

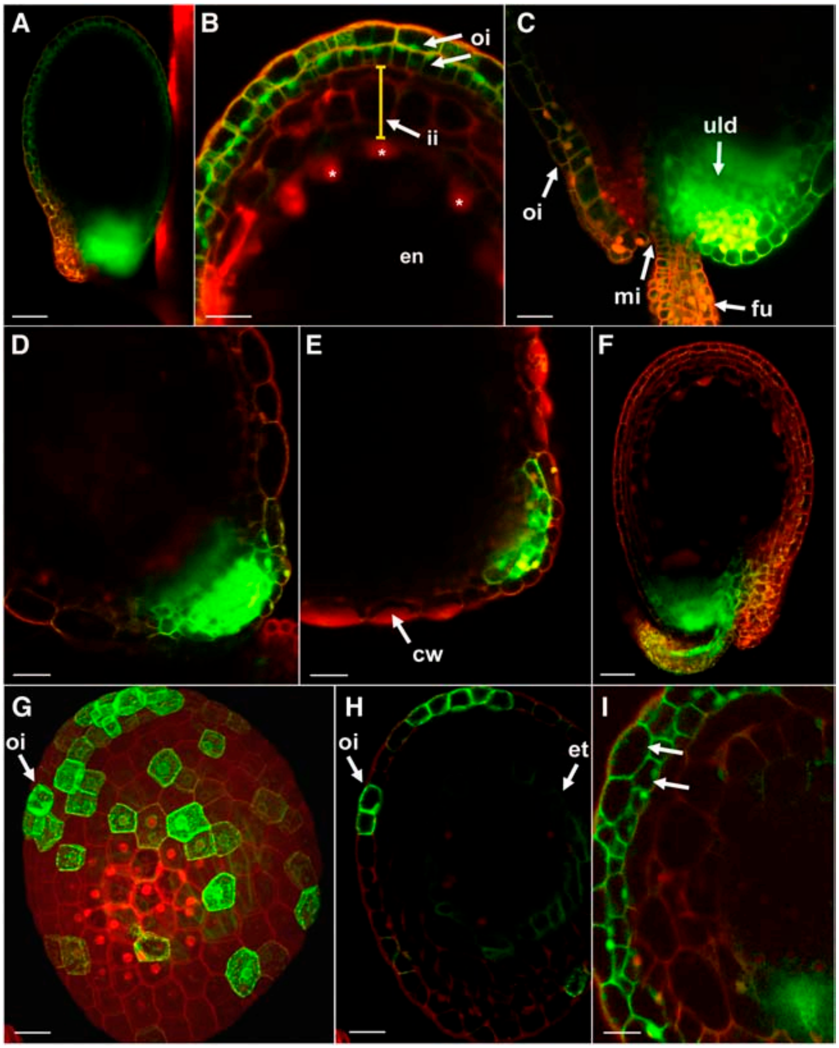

Figure 1. Analysis of the symplastic connectivity and of post-phloem GFP movement in the outer integument of Arabidopsis seeds. A to E, Seeds from *AtSUC2* promoter/*GFP* plants. A, Overview of the GFP fluorescence in a seed from the fifth silique (2 d old; globular stage of the embryo; bar = 50 μm). B, Magnification of the tip region of a seed similar to that shown in A. GFP fluorescence is detected in both cell layers of the outer integument (oi). No GFP fluorescence is seen in any of the three cell layers of the inner integument (ii; yellow bar) or in the endosperm (en). Some of the peripheral endosperm nuclei are marked with asterisks (bar = 25 μm). C, Magnification of the basal unloading (uld) domain at the end of the funiculus (fu) of a seed similar to that shown in A. Weak GFP fluorescence is seen in both cell layers of the outer integument (oi; mi, micropyle; bar = 25 μm). D, GFP fluorescence in a seed from the twelfth silique (6 d old; upturned-U stage of the embryo). At this stage, GFP is still unloaded from the funicular vascular bundle, but post-phloem movement of GFP in the outer integument is no longer detected (bar = 25 μm). E, GFP fluorescence in a seed from the fifteenth silique (10 d old; mature embryo). GFP fluorescence is seen only in few cells of the unloading domain. At this stage, cell wall (cw) thickening and development of the testa have already started (bar = 25 μm). F, Seed from an *AtSUC2* promoter/*GFP*-sporamin plant. GFP-sporamin is unloaded from the vascular bundle at the end of the funiculus, but post-phloem movement in the outer integument is not detected (2 d old; globular stage of the embryo; bar = 40 μm). G and H, Seed from an *AtGL2* promoter/*tmGFP9* plant. G, View of the seed from the outside showing *AtGL2* promoter activity in individual cells of the outer integument (oi; bar = 20 μm). H, Optical section through the seed shown in G confirming the *AtGL2* promoter activity in the outermost cell layer of the outer integument (oi). A weak activity of the *AtGL2* promoter is also seen in the innermost layer of the inner integument, the endothelium (et; bar = 20 μm). I, Seed of an *AtGL2* promoter/*GFP* plant. GFP fluorescence is seen in both layers of the outer integument (arrows) showing that GFP can move cell to cell not only within the outer cell layer but also from the outer into the inner cell layer (bar = 25 μm). All images represent CLSM images. G is a maximum projection of a picture stack. All others represent optical sections. Red color results from propidium iodide staining of cell walls.

Arabidopsis seed (Fig. 1, A–C). No movement of GFP was observed from these two layers or from the unloading domain into the underlying layers of the inner integument (Fig. 1B). This demonstrates that the cells of the outer integument are connected by plasmodesmata with a large SEL (at least 27 kD [GFP]; see "Discussion") and that these cells form a single symplast. Phloem unloading of GFP into Arabidopsis seeds was compared in siliques at different developmental stages (Fig. 1C, silique no. 5 [2 d old; globular stage of the embryo]; Fig. 1D, silique no. 12 [6 d old; upturned-U stage of the embryo]; Fig. 1E, silique no. 15 [10 d old; mature embryo; see "Materials and Methods"]). Clearly, the extent of GFP unloading decreases during seed maturation, and in silique number 15 (mature embryo), where seed development is almost complete and the outer integument starts to develop the thick-walled testa, GFP is detected only in very few cells at the seed base.

Phloem unloading was also studied in seeds of Arabidopsis plants expressing the ORF for a GFP-sporamin fusion protein (Stadler et al., 2005) under the control of the *AtSUC2* promoter (47 kD). Figure 1F shows that the GFP-sporamin fusion is unloaded at the funicular end of the phloem into the unloading domain of the seed like the unfused GFP. However, in contrast to GFP, no post-phloem movement was observed for the 47-kD GFP-sporamin. This lack of GFP-sporamin movement was independent of the developmental stage of the ovule, which demonstrates that the SEL of the cells of the Arabidopsis outer integument allow macromolecular movement of globular proteins of up to 27 kD, but not of the 47-kD protein. Moreover, the plasmodesmal SEL between the cells of the outer integument is smaller than that of the cells in the unloading domain.

Clearly, GFP fluorescence observed in the two cell layers of the outer integument in *AtSUC2* promoter/*GFP* plants (Fig. 1, B and C) results from the lateral diffusion of GFP from the unloading domain into these two layers. However, these data do not show whether movement of GFP can also occur between these two cell layers (i.e. from the outer into the inner cell layer or vice versa). To this end, the analyses of post-phloem GFP movement in the outer integument were extended to transgenic Arabidopsis lines expressing the ORFs for GFP or for a membrane-targeted GFP variant (tmGFP9; Stadler et al., 2005) directly in one of the two cell layers of the outer integument. In contrast to the freely mobile GFP, the membrane-anchored tmGFP9 fusion cannot move cell to cell because GFP is fused to the C terminus of six transmembrane helices of the monosaccharide transporter AtSTP9 (Schneidereit et al., 2003; Stadler et al., 2005). The ORFs for these fluorescent probes were expressed under the control of the Arabidopsis *GLABRA 2* (*AtGL2*) promoter that is known to be active in the outer cell layer of the outer integument (Windsor et al., 2000), as well as in roots (Masucci et al., 1996) and in leaves and trichomes (Szymanski et al., 1998).

Our analyses of *AtGL2*-dependent tmGFP9 fluorescence in the outer integument confirm previous reports on the activity of this promoter in the outermost cell layer of the testa (Windsor et al., 2000). No *AtGL2* promoter activity was observed in the inner cell layer of the outer integument (Fig. 1, G and H). However, there were two new and unexpected observations: (1) the *AtGL2* promoter drives expression of *tmGFP9* only in distinct cells of the outer cell layer in the outer integument, whereas other cells do not show any detectable tmGFP9 fluorescence (Fig. 1, G and H); and (2) weak activity of the *AtGL2* promoter was also detected in the innermost cell layer of the inner integument, the endothelium (Fig. 1H). In contrast, the fluorescence patterns of GFP in *AtGL2* promoter/*GFP* plants (Fig. 1I) showed GFP fluorescence in both cell layers of the outer integument. This confirms the results obtained with *AtSUC2* promoter/*GFP* plants (Fig. 1B) showing that the cells of the outer integument form a symplastic domain and are connected by plasmodesmata with a dilated aperture. In addition, these data show that macromolecules, such as GFP, can move symplastically not only within the outer layer of the outer integument but also centripetally, i.e. from the outer cell layer into the inner cell layer of the outer integument (and probably also in the opposite direction). As in Fig. 1B, no movement of GFP could be observed into the inner integument (Fig. 1H).

All Cells of the Inner Integument Form a Symplastic Continuum and Are Connected by Plasmodesmata with a Dilated Aperture

The symplastic connectivity between the cells of the inner integument was analyzed in transgenic Arabidopsis plants expressing the ORFs of *GFP* or *tmGFP9* under the control of the Arabidopsis *TRANSPARENT TESTA 12* (*AtTT12*) promoter. *AtTT12* encodes a multidrug transporter-like protein and is expressed in the endothelium, the innermost cell layer of the testa (Debeaujon et al., 2001). The fluorescence pattern observed in *AtTT12* promoter/*tmGFP9* plants confirmed the published promoter activity in this cell layer (Fig. 2A). In contrast, the GFP fluorescence in *AtTT12* promoter/*GFP* plants showed that free GFP can move symplastically from the endothelium into the adjacent, middle cell layer of the inner integument and even into the outermost cell layer adjacent to the outer integument (Fig. 2B). This shows that all cells of the inner integument do form a symplastic domain and are connected by plasmodesmata with a dilated aperture, allowing the macromolecular movement of proteins of at least up to 27 kD.

Outer and Inner Integument Share Few or No Functional Plasmodesmata

The results presented so far suggest that the cell wall between the innermost cell layer of the outer integument and the outermost cell layer of the inner

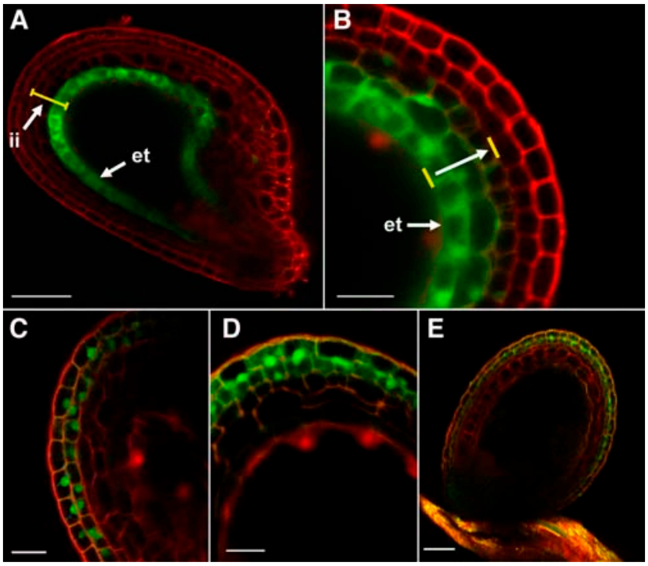

Figure 2. Analysis of the symplastic connectivity between the inner and outer integuments of Arabidopsis seeds. A and B, Analysis with *AtTT12* promoter/*tmGFP9* plants. C to E, Analysis with HPTS. A, Seed of an *AtTT12* promoter/*tmGFP9* plant. The fluorescence of the membrane-bound GFP is restricted to the endothelium (et). No tmGFP9 fluorescence is detected in the two other cell layers of the inner integument (ii; yellow bar; bar = 50 μm). B, Seed of an *AtTT12* promoter/*GFP* plant. Strong GFP fluorescence is seen in the endothelial (et) layer, where the *AtTT12* promoter is active (see A), but clearly GFP can diffuse into the two adjacent cell layers (direction of the white arrow). The two yellow bars show the inner and outer borders of the inner integument (scale bar = 20 μm). Both images represent optical sections (CLSM). Red color results from propidium iodide staining of cell walls. C, Optical section through an Arabidopsis wild-type seed 120 min after HPTS loading (bar = 20 μm). D, Optical section through an Arabidopsis wild-type seed 4 h after HPTS loading (bar = 20 μm). E, Optical section through an Arabidopsis wild-type seed 5 h after HPTS loading (bar = 50 μm). All images represent CLSM images. All images represent optical sections. Red color results from propidium iodide staining of cell walls.

integument has either no plasmodesmata or plasmodesmata with a less- dilated aperture that prevent movement of GFP between the integuments. We tested these two possibilities in dye-loading experiments with the low-M_r fluorescent probe HPTS and followed the distribution of these dyes by CLSM. HPTS has previously been used as a symplastic probe, can be applied via Arabidopsis leaves, is loaded into the phloem and distributed to the different sink tissues with the flow of assimilates, and eventually is symplastically unloaded (Wright and Oparka, 1996).

In HPTS-loaded plants, fluorescence was found in both layers of the outer integument quite early (Fig. 2C; 120 min) and HPTS stayed in the outer integument also after a prolonged supply (Fig. 2, D [4 h] and E [5h]). HPTS fluorescence in the inner integument was detected only occasionally and, even in these rare cases, the fluorescence stayed much stronger in the outer than in the inner integument. Our data on the movement of low-M_r fluorescent probes demonstrate that, in fact, plasmodesmata seem to be absent or scarce in the walls between the inner and outer integument. The nonmembrane-permeable dye HPTS showed no movement across this border.

The Suspensor Forms a Symplastic Continuum with the Globular Stage Embryo

After fertilization of the egg cell, the polarized zygote divides into two cells with the basal cell that is adjacent to the micropylar end of the seed forming the suspensor. This structure has repeatedly been shown to promote growth of in vitro cultured embryos and to represent the major route of nutrient uptake and an important source for growth regulators for globular and heart-stage embryos (for review, see Yeung and Meinke, 1993). Uptake of ^{14}C-Suc by suspensors of Phaseolus was shown to be sensitive to uncouplers (Yeung, 1980), but promotion of embryo growth was said to occur by facilitated diffusion (Yeung and Meinke, 1993).

To determine the possible mode of nutrient supply and growth regulator movement from the suspensor into the embryo and vice versa, we expressed the ORFs of *GFP* and *tmGFP9* in the suspensor of Arabidopsis embryos using the promoter of the Arabidopsis Suc-transporter gene *AtSUC3* that was known to be active in several sinks, including the suspensor (Meyer et al., 2004). As previously described, tmGFP9 fluorescence was seen exclusively in the suspensor in *AtSUC3* promoter/*tmGFP9* plants (Fig. 3A). In contrast, in *AtSUC3* promoter/*GFP* plants, fluorescence was seen in the suspensor as well as the embryo, indicating that GFP can move from the suspensor into the globular embryo and that the suspensor and the early embryo form a single symplast.

GFP Can Move from the Embryo Epidermis into the Inner Embryo Cell Layers, But Mobility of GFP Is Reduced during Embryo Development

Numerous auxin-regulated genes, such as *PIN-FORMED1* (*PIN1*), *PIN4*, *PIN7*, *MONOPTEROS*, *BODENLOS* (*BDL*), *REVOLUTA*, *PHAVOLUTA*, *MERISTEM LAYER1*, and others, are known to show promoter activity in specific cells of the early globular, late globular, and triangular stages of Arabidopsis embryos (for review, see Weijers and Jürgens, 2005). Interestingly, in several cases, the site of gene expression is different from the site of protein action (Berleth and Jürgens, 1993; Hamann et al., 1999), indicating non-cell-autonomous regulatory mechanisms. The movement of GFP from the suspensor into all cells of the early globular embryo (Fig. 3, A and B) suggests a possible cell-to-cell movement not only for hormones such as auxin, but also for regulatory proteins, such as indole-3-acetic acid 12 (encoded by *BDL*) that has an apparent molecular mass of 26.3 kD and is therefore in the same size range as GFP, with a mass of 27 kD. In fact, only recently Kim and coworkers (2005) reported that the embryo constitutes a single symplast because GFP

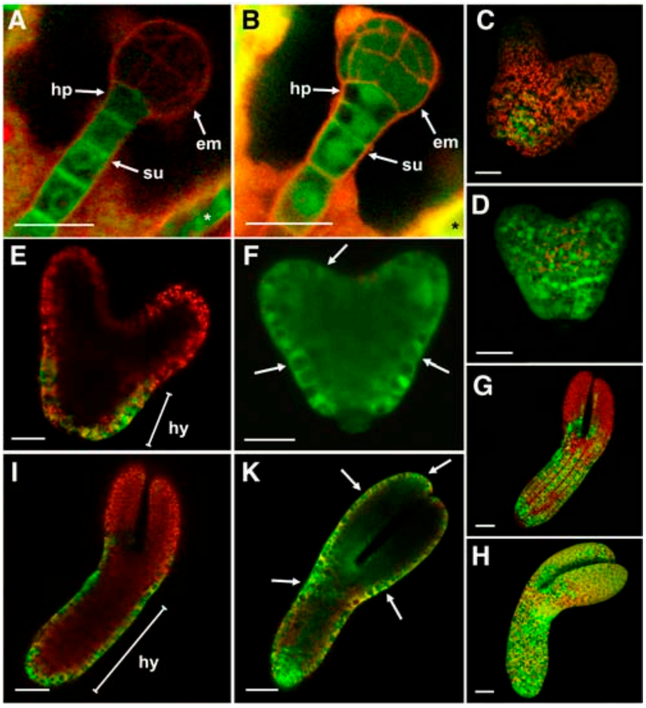

Figure 3. Symplastic connectivity in the suspensor and the developing Arabidopsis embryo. A, Globular stage embryo (em) and suspensor (su) of an *AtSUC3* promoter/*tmGFP9* plant. Green tmGFP9-derived fluorescence is detected in all cells of the suspensor and in the hypophysis (hp). The asterisk marks the endothelium, where the *AtSUC3* promoter is also active (bar = 25 μm). B, Globular stage embryo (em), hypophysis (hp), and suspensor (su) of an *AtSUC3* promoter/*GFP* plant. In contrast to A, green GFP-derived fluorescence is detected also in all cells of the embryo. The asterisk marks the endothelium, where the *AtSUC3* promoter is also active (bar = 25 μm). C, View of an intact early heart-stage embryo of an *AtGL2* promoter/*tmGFP9* plant showing tmGFP9 fluorescence only in distinct cells in the hypocotyl region (bar = 20 μm). D, View of an intact early heart-stage embryo of an *AtGL2* promoter/*GFP* plant showing GFP in all cells. Bright green dots show GFP accumulation in nuclei (bar = 20 μm). E, Optical section of the embryo shown in C showing that tmGFP9 fluorescence is restricted to the hypocotyl (hy) epidermis (bar = 20 μm). F, Optical section of the embryo shown in D showing GFP in all epidermis cells (arrows), but also in all underlying cell layers (bar = 20 μm). G, View of a midtorpedo-stage embryo of an *AtGL2* promoter/*tmGFP9* plant. tmGFP9 fluorescence is seen only in rows of cells in the hypocotyl and the lower part of the cotyledons (bar = 40 μm). H, View of an intact midtorpedo-stage embryo of an *AtGL2* promoter/*GFP* plant. GFP fluorescence is seen in all cells (bar = 40 μm). I, Optical section of the embryo shown in G showing that tmGFP9 fluorescence is restricted to the hypocotyl (hy) epidermis (bar = 40 μm). K, Optical section of the embryo similar to that shown in H showing strong GFP fluorescence in all cells of the epidermis (arrows) and in the root tip. GFP can still move into the underlying cell layers of the embryo, but movement into these cells is clearly reduced compared to the heart-stage embryo shown in F (bar = 40 μm). All images represent CLSM pictures. C, D, G, and H are maximum projections of picture stacks; all others represent optical sections. Red color shows propidium iodide-stained cell walls in A and B and chlorophyll autofluorescence in all other images.

synthesized under the control of a meristem-specific promoter moved into all cells of developing embryos.

We analyzed the capacity of GFP to move cell to cell in embryos in early heart- (Fig. 3, C–F) and midtorpedo-stage embryos (Fig. 3, G–K) in Arabidopsis *AtGL2* promoter/*tmGFP9* and in *AtGL2* promoter/*GFP* plants. Figure 3, C and E (early heart stage), and Figure 3, G and I (midtorpedo stage), show that *tmGFP9* is expressed only in distinct cells in the epidermis in the embryo hypocotyl. Consequently, no tmGFP9 fluorescence is seen in the cotyledons or in subepidermal layers of these embryos. In contrast, free GFP moves into all cells of the early heart-stage embryo (Fig. 3, D and F) showing that, at this stage, the embryo is still one large symplastic continuum. However, GFP movement within the epidermis seems to be more rapid than the movement from the epidermis into the inner embryo because stronger GFP fluorescence is detected in all epidermis cells of the embryo. This was even more obvious in midtorpedo-stage embryos, where GFP can still move from the epidermis into all inner cells (Fig. 3K); however, this centripetal movement of GFP out of the epidermis is clearly less efficient than GFP movement within the epidermis (Fig. 3, H, and arrows in K).

This observation was confirmed by a quantification of the GFP fluorescence in three different areas (epidermis where the *AtGL2* promoter is active, epidermis where the *AtGL2* promoter is not active, and ground

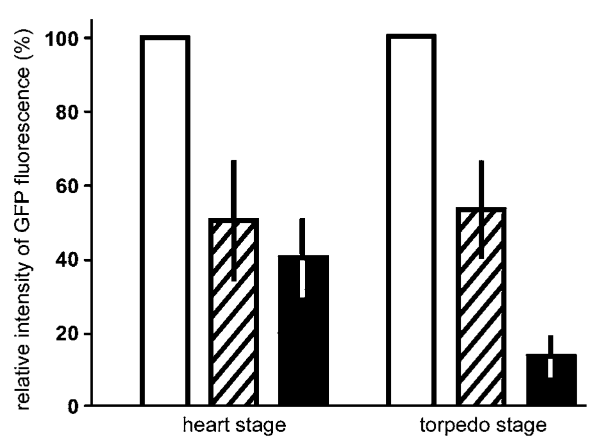

Figure 4. Quantification of the intensity of GFP fluorescence in different areas of heart-stage and torpedo-stage embryos of *AtGL2* promoter/*GFP* plants. The GFP fluorescence (497–526 nm; mean ± SD) from four to six images was determined in three different areas by integration. The selected areas were (1) epidermis from the hypocotyl (white bars), where the *AtGL2* promoter is known to be active (see Fig. 3, E and I); (2) epidermis from the emerging cotyledons (hatched bars), where the *AtGL2* promoter was shown not to be active (see Fig. 3, E and I); and (3) ground tissue cells from the emerging cotyledons (black bars). All values were normalized to the same area and the intensity at the site of *AtGL2* promoter activity was always set to 100%. The hatched bars show that the intensity of GFP movement within the epidermis is the same in heart-stage and in torpedo-stage embryos. The black bars demonstrate that movement of GFP from the epidermis into the underlying ground tissue is reduced by a factor of 3 during the transition from heart stage to torpedo stage.

tissue) of heart-stage and torpedo-stage embryos from *AtGL2* promoter/*GFP* plants (Fig. 4). The extent of GFP movement within the epidermis is not altered during the transition from heart stage to torpedo stage. In contrast, GFP movement into the underlying ground tissue, which is comparable to the movement within the epidermis in heart-stage embryos, is reduced by a factor of 3 in torpedo-stage embryos.

Formation of Symplastic Units during Embryo Development

The data shown so far demonstrate that although GFP can, in principle, move from the epidermis into all cells of the embryo, the symplastic connectivity between the epidermis and the underlying cell layers seems to be continuously reduced during embryo development. In contrast, the connectivity between the individual cells of the epidermis stays high. This suggests that, in the midtorpedo stage, symplastic units start to develop first in the Arabidopsis embryo.

To study in more detail the possibility of symplastic units forming first at this stage, we analyzed the distribution of free GFP in embryos of *AtSUC3* promoter/*GFP* plants. First, it was shown in Figure 3, A and B, that GFP synthesized in the suspensor can move into globular-stage embryos. We were interested to see whether this movement is also maintained in older embryos. Second, we had observed that the *AtSUC3* promoter is active in distinct cells of embryos starting at the midtorpedo stage. We studied the movement of GFP out of these cells.

Figure 5A shows an optical section through a triangular-stage embryo from an *AtSUC3* promoter/*GFP* plant. As in the globular stage (Fig. 3A), the *AtSUC3* promoter is active in the suspensors of this embryo. However, at this stage no movement of GFP from the suspensor into the embryo or into the hypophysis can be observed. This demonstrates that, during the transition from globular stage to heart stage, the symplastic connectivity between suspensor and embryo hypophysis is reduced.

Figure 5, B to E, shows Arabidopsis embryos in the torpedo stage with *AtSUC3* promoter activity in the root. In *AtSUC3* promoter/*tmGFP9* embryos, the resulting tmGFP9 fluorescence is restricted to the outermost cell layer of the root tip (Fig. 5, B and C), whereas free GFP can move into the hypocotyl in *AtSUC3* promoter/*GFP* embryos (Fig. 5, D and E). This supports the conclusion drawn from the results shown in Figure 3, indicating that GFP can move freely within the embryo.

Figure 6, F to L, shows almost fully developed embryos from *AtSUC3* promoter/*tmGFP9* plants (Fig. 6, F–H) or from *AtSUC3* promoter/*GFP* plants (Fig. 5, I–L). At this stage, the *AtSUC3* promoter is still active in the root tip, but additional *AtSUC3* promoter activity is seen in individual cells of the cotyledons (Fig. 5, H and L). The fluorescence in the root tip is restricted to the outermost cell layer in *AtSUC3* promoter/*tmGFP9*

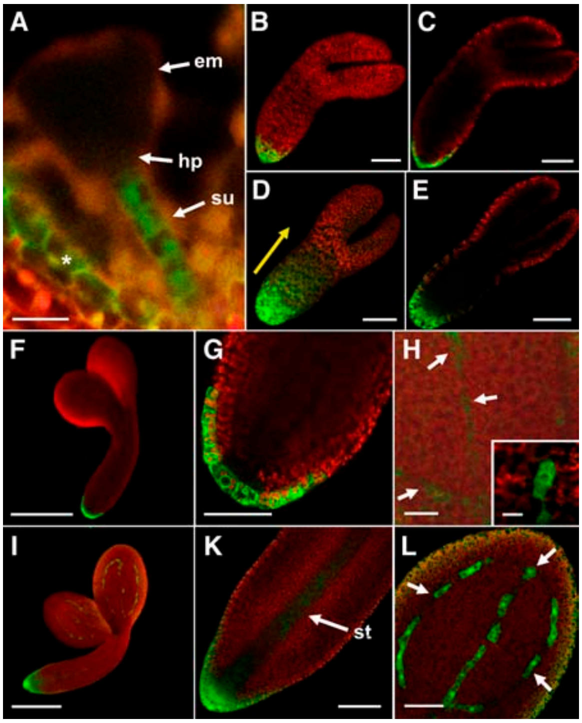

Figure 5. Initiation and formation of symplastic units during embryo maturation. A, Optical section through a triangular stage embryo (em) of an *AtSUC3* promoter/*GFP* plant. GFP fluorescence is seen in the endothelial layer of the inner integument (asterisk) and in the suspensor (su). Movement of GFP from the suspensor into the embryo or the hypophysis (hp) is no longer detected at this stage (bar = 25 μm). B and C, Confocal projection (B) or optical section (C) of an *AtSUC3* promoter/*tmGFP9* embryo in the midtorpedo stage. B, View of the intact embryo. tmGFP9 fluorescence is seen only in the root tip (bar = 50 μm). C, tmGFP9 fluorescence is restricted to the root-tip epidermis (bar = 50 μm). D and E, Confocal projection (D) or optical section (E) of an *AtSUC3* promoter/*GFP* embryo in the midtorpedo stage. D, View of the intact embryo shows a gradient of GFP diffusing from the root tip toward the apex (yellow arrow; bar = 50 μm). E, GFP does move from the root-tip epidermis into the adjacent cell layers of the embryo, but, as in Figures 3K and 5D, diffusion seems to be better within the epidermis (bar = 50 μm). F to H, View from the outside (confocal projection) of the almost mature embryo of an *AtSUC3* promoter/*tmGFP9* plant (F) or optical sections from the embryo root tip (G) or the cotyledon (H). F, tmGFP9 fluorescence is seen only in the root tip. The fluorescence shown in H is weaker than that in the root tip and is not seen in this image (bar = 200 μm). G, tmGFP9 fluorescence is confined to the epidermis of the root tip (bar = 50 μm). H, tmGFP9 fluorescence is seen in individual cells of the cotyledon (arrows). Due to the low expression of tmGFP9 in these cells, the cell borders are difficult to visualize. The inset shows a single cell at slightly higher magnification (bar = 25 μm; inset, 10 μm). I to L, View from the outside (confocal projection) of the almost mature embryo of an *AtSUC3* promoter/*GFP* plant (I) or optical sections from the embryo root tip (K) or the cotyledon (L). I, GFP fluorescence is seen in distinct cells of the cotyledons and in the root tip (bar = 200 μm). K, GFP can move from the cells of the root-tip epidermis into all adjacent cells, but movement of GFP is seen primarily in the developing stele (st) in the center of the hypocotyl (bar = 50 μm). L, GFP fluorescence is seen in individual cells on the cotyledon (arrows). No movement of GFP out of these cells can be detected (bar = 50 μm). Red color shows chlorophyll autofluorescence in all images.

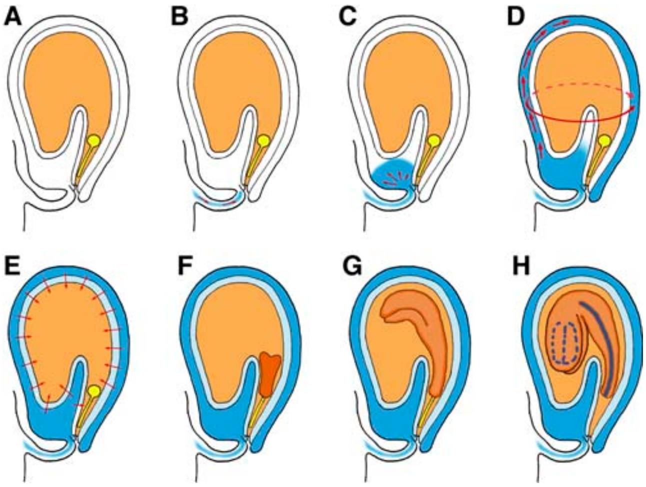

Figure 6. Model showing the symplastic domains in a developing Arabidopsis seed and the deduced path of assimilates. A, All maternal tissues of the seed are shown in white, the endosperm in light orange, and the suspensor and the embryo in yellow. B, Flux of assimilates in the vascular bundle of the funiculus. This bundle ends in the testa proximal to the micropyle. C, Unloading into the post-phloem unloading domain. D, Movement within the outer integument (red arrows), which forms a symplastic extension of the vascular tissue. E, Centripetal transport (red arrows) from the outer integument toward the endosperm over two apoplastic borders. In the young seed, the suspensor and the embryo form a single symplastic domain (Fig. 3, A and B). F, During the early heart stage. the symplastic continuity between embryo and suspensor is interrupted (Fig. 5A) and the embryo forms a single symplastic domain. G, During the transition from heart to midtorpedo stage, the symplastic connectivity between epidermis and inner cell layers of the embryo is gradually reduced. The symplastic connectivity between the cells of the epidermis is high. H, In mature embryos, the developing stele in the root and the hypocotyl begins to form an independent domain. Cells within the stele show high symplastic connectivity, allowing the movement of GFP synthesized in the root-tip epidermis (Fig. 5, F and G). The symplastic connectivity between developing stele and root cortex is low and significant movement of GFP out of the stele is not observed. At the same time, individual cells along the leaf vascular bundles show reduced symplastic connectivity to their adjacent cells. GFP synthesized in these cells (Fig. 5H) does not move out of these cells (Fig. 5L).

plants (Fig. 5G) as in the younger embryo stages (Fig. 5, B and C). In *AtSUC3* promoter/*GFP* plants, GFP does again move into all adjacent cells, but, in contrast to the younger embryo stages, movement of GFP is seen primarily in cells in the center of the hypocotyl, most likely the developing stele (Fig. 5K).

A comparison of the fluorescence patterns in the embryo cotyledons shown in Figure 5H (tmGFP9) and in Figure 5L (GFP) shows that, in both cases, individual cells fluoresce. Surprisingly, free GFP does not move out of these cells in *AtSUC3* promoter/*GFP* plants, suggesting that these cells are connected to their neighbor cells by plasmodesmata with a closed or less dilated aperture. These green fluorescent cells form a pattern (Fig. 5, H and L) that resembles that of the vascular tissue in mature cotyledons (Truernit and Sauer, 1995). However, the size of these cells and the fact that they do not form a continuous file of labeled cells show that they do not represent parts of the developing vasculature. Rather, they look like individual, large cells (S cells) that are known to express *AtSUC3* and that were shown to be in close proximity to the vasculature in mature Arabidopsis leaves (Koroleva et al., 2000; Meyer et al., 2000, 2004).

In summary, the data presented demonstrate that, during the late stages of embryo development, the symplastic connectivity is gradually reduced between individual cells or between groups of cells that are about to form future tissues (epidermis or stele). In the mature or almost mature embryo, symplastic units (or symplastic domains) are formed first, which separate symplastically from the rest of the embryo and are no longer connected to their neighbor cells by plasmodesmata with a dilated aperture.

DISCUSSION

Developing seeds of higher plants are complex structures that are composed of a set of different sink tissues cooperating to feed and shelter the growing embryo. This article (1) dissects the symplastic domains in developing Arabidopsis seeds; (2) identifies apoplastic borders, where carrier-mediated transport has to be postulated; and (3) describes the modulation of symplastic connectivities between defined cells and cell clusters in the developing embryo.

The SEL of Plasmodesmata

There is no direct relationship between the molecular masses and the molecular dimensions of different molecules. For example, a 25-kD dextran and a 51-kD globular protein both have the same R_S (3.0 nm; Oparka and Santa Cruz, 2000). Therefore, the size of moving molecules should ideally be given in terms of molecular dimension (nm) and not in terms of molecular mass (kD). This is possible for more-or-less ball-shaped molecules like dextrans (Jorgensen and Møller, 1979) or globular proteins (Le Maire et al., 1986). For GFP, R_S values of 2.8, 2.35, or 2.6 nm were deduced from its translational diffusion coefficient (Terry et al., 1995), from gel filtration experiments (Ribbeck and Görlich, 2001), or from cell-to-cell mobility assays (Fisher and Cash-Clark, 2000a; average R_S = 2.6 nm).

In contrast to free GFP, however, the GFP-sporamin fusion (47 kD) used in this and other articles (Hoth et al., 2005; Stadler et al., 2005) represents a fusion of two globular proteins with individual R_S values (2.6 nm for GFP and 2.0 nm for sporamin; deduced from Le Maire et al., 1986). A precise molecular dimension can, therefore, neither be given for GFP-sporamin nor for other fusions used in similar analyses (e.g. dimerized GFP [Kim et al., 2005] or GFP-ubiquitin or GFP-patatin [Stadler et al., 2005]). For this reason, we mostly refer to the SEL of plasmodesmata in kilodaltons rather than in nanometers.

The Outer Integument Is a Post-Phloem Extension of the Vascular Tissue

GFP synthesized in the CCs is released at the end of the single vascular strand of the funiculus into a set of cells at the seed base (Fig. 6, A and B). This unloading is also seen for GFP-sporamin, which does move from the vascular bundle of the funiculus into the same cells (Fig. 1F). The observation that only GFP (27 kD), but not the GFP-sporamin fusion (47 kD), can move from this unloading zone into the other cells of the outer integument resembles the phloem unloading in Arabidopsis root tips (Stadler et al., 2005). In both cases, the 47-kD fusion protein is unloaded from the phloem into a small set of cells, and, in both cases, only the 27-kD protein can move from these cells into the adjacent sink organ, i.e. into the root tip (Stadler et al., 2005) or into the outer integument (this article). This suggests a common mechanism of phloem unloading in both terminal sinks and the existence of discrete unloading domains with similar SELs (at least 47 kD) in both cases. Interestingly, unloading of even larger molecules (400-kD dextran) has been reported in wheat grains (Fisher and Cash-Clark, 2000a). It will be necessary to analyze Arabidopsis lines expressing larger GFP fusions to see whether unloading of these molecules is also possible from the funicular phloem. Fisher and Cash-Clark (2000a) reported also that the largest molecules showing post-phloem transport in wheat grains were 16-kD dextrans with an R_S of 2.6 nm. As mentioned above, GFP has about the same R_S, indicating that the SEL of plasmodesmata in the post-phloem path is similar in wheat and in Arabidopsis.

The movement of unloaded GFP into all cells of the outer integument, and its movement from the outer cell layer of the outer integument into the inner cell layer of the outer integument in *AtGL2* promoter/*GFP* plants (Fig. 1I), demonstrates that all cells of both cell layers of the outer integument form a single symplast and that all these cells are connected by plasmodesmata with a dilated aperture (SEL at least 2.6 nm or 27 kD protein), thus forming a symplastic post-phloem extension of the funicular phloem.

Identification of Apoplastic Borders

The fact that neither GFP (Fig. 1, A–C) nor the low-M_r dye HPTS (Fig. 2, C–E) can move from the outer into the inner integument shows that the two integuments are not connected by functional plasmodesmata or at least not by a significantly large number. The movement of GFP within the inner integument of *AtTT12* promoter/*GFP* plants (Fig. 2, A and B) demonstrates that all three cell layers of this integument also constitute a single symplast. This observation and the fact that the endosperm, which is next to the inner integument, is a syncytium and cellularizes quite late in its development (Otegui and Staehelin, 2000) shows that there are only three apoplastic borders between the phloem and the embryo: (1) between the outer and inner integument; (2) between the inner integument and the endosperm; and (3) between the endosperm and the embryo. Only for these apoplastic steps does a carrier-mediated transport (e.g. for Suc or amino acids) seem necessary. In the case of Suc, these transport steps could, for example, be catalyzed by the Suc transporters AtSUC3 and AtSUC5, which are present in the cell layers adjoining these apoplastic gaps (AtSUC3 in specific cell layers of the integuments and in the suspensor [Meyer et al., 2004] and AtSUC5 in the endosperm and in the embryo [A. Ludwig and N. Sauer, unpublished data]).

The importance of symplastic post-phloem transport in the testa has previously been described by several other groups (for review, see Patrick and Offler, 2001). However, all plants used in these analyses (grain legumes and cereals) possess a vascular compartment in their testa and the photoassimilates move symplastically from the testa phloem into the seed coat symplast. Eventually, specialized cells of this symplast release the photoassimilates into the seed apoplast (Patrick and Offler, 1995; Wang et al., 1995). An apoplastic border within the testa has not been observed in these plants.

We speculate that, in Arabidopsis, the outer integument functions as a symplastic extension of the funicular phloem, with a physiological role that is similar to that of the vascular compartment in the testa of cereals and grain legumes (import of photoassimilates into the testa). In contrast, the function of the Arabidopsis inner integument is similar to that of the ground tissue or of the seed coat symplast in grain legumes and cereals (transit of photoassimilates to the inner surface and release from the testa; Fig. 6, D and E). The main difference is that there is no symplastic connection between the inner and outer integument in Arabidopsis. In contrast, the vascular compartment of the testa is symplastically connected directly to the symplastic compartment that is responsible for the release of photoassimilates to the seed apoplast (Patrick and Offler, 2001).

Symplastic Domains in the Developing Embryo

After the uptake of nutrients by plasma membrane transporters of the suspensor (e.g. of Suc by AtSUC3; Fig. 3A), these substances have to be delivered to the growing embryo. In fact, it is generally assumed that the suspensor has a nutritive function for the young embryo (Yeung and Meinke, 1993). However, this function is most likely limited to the early steps of embryo development because, in Arabidopsis, the suspensor begins to degenerate around the heart stage of embryo development (Meinke, 1994). Nothing was known about possible symplastic connections between the suspensor and, if present, how or when such connections might be closed prior to the degeneration of the suspensor. Figure 3, A and B, demonstrates that the embryo and the suspensor form, in fact, a single symplast in the globular stage of embryo development. The plasmodesmata connecting the suspensor to the embryo and the embryo cells with each other allow the movement of GFP and have, therefore, a SEL of at least 2.6 nm. However, already during the triangular stage of embryo development, the SEL of the plasmodesmata connecting the hypophysis and the adjacent cell of the suspensor is reduced, and GFP synthesized in the suspensor can no longer move into the hypophysis or the embryo (Fig. 5A). Obviously, the symplastic connectivity between suspensor and embryo changes well before the initiation of suspensor degradation. Interestingly, this symplastic disconnection of the suspensor from the hypophysis and the embryo coincides in time with the specification of the hypophysis. This occurs in response to an auxin signal from the embryo (Weijers and Jürgens, 2005), and mutants that fail to specify the hypophysis at this stage (*monopteros* and *bdl*; Berleth and Jürgens, 1993; Hamann et al., 1999) do not make an embryonic root. The observed change in the symplastic connectivity of hypophysis plasmodesmata may play an important role in this developmental step.

Up to this stage, the embryo constitutes a single symplast (Kim et al., 2005; this article) and nutrients, signaling molecules, hormones, and even small peptides can move quite freely from one cell to the other. However, beginning with the heart stage and even more pronounced in the torpedo stage, GFP starts to move better or preferentially between certain cell types (e.g. within the epidermis [Figs. 3, F and K, and 4] or from the root tip into the stele [Fig. 5K]) and less good between others (e.g. from the epidermis into the underlying cells [Figs. 3, F and K, and 4]). This suggests that either the number of plasmodesmata or their SEL is gradually reduced during embryo development and during the onset of tissue differentiation. During the final steps of embryo maturation, individual cells can be labeled even with freely mobile GFP (Fig. 5, H and L), demonstrating that, at this stage, the free movement of macromolecules is no longer possible between all cells of the embryo.

Kim and coworkers (2005) suggested that the embryo is a single symplast at all developmental stages, and large symplastic domains have also been described in the filial tissues of grain legume seeds (for review, see Patrick and Offler, 2001). Our results demonstrate the formation of new symplastic domains during embryo maturation in Arabidopsis and the partial uncoupling of these domains from neighbor domains (Figs. 3, G and K, and 5K). In some cases, macromolecular cell-to-cell movement even stops completely (Fig. 5L). This shows that the formation of symplastic domains can be visualized in the developing embryo and that it coincides with the beginning differentiation of certain cells or tissues (e.g. epidermis, vasculature, and S cells). It also demonstrates, however, that the site of GFP synthesis plays an important role in whether or not its movement can be detected. Obviously, synthesis of GFP from a synthetic promoter and movement of GFP within the entire ground tissue (Kim et al., 2005) make it difficult to detect individual cells that are not connected to this symplast.

The symplastic domains described in our analyses and also the large SELs of their plasmodesmata may not only be important for directing and regulating the flow of assimilates, but also may contribute to correct morphogenesis, e.g. by allowing the movement of transcription factors (Lucas et al., 1995; Sessions et al., 2000; Nakajima et al., 2001; Wu et al., 2003) or RNAs (Ruiz-Medrano et al., 1999; Xoconostle-Cazares et al., 1999). With this in mind, and with the data on the movement of GFP in Arabidopsis embryos (Kim et al., 2005; this article), it is surprising that, in globular or heart-stage Arabidopsis embryos, an apical-to-basal flow is described for the low-M_r phytohormone auxin that is exclusively in the apoplast (Friml et al., 2004; Blilou et al., 2005). It has been postulated that this flow occurs by alternating export of auxin from one cell and import of auxin by a transporter-mediated polar auxin transport. Our data and the data of Kim et al. (2005) would suggest, rather, that auxin, once it is inside the embryo symplast, would move cell to cell quite efficiently. Therefore, it is also difficult to imagine how auxin could act as a signaling molecule only in the terminal cell, the hypophysis, and not in all cells on its way (Friml et al., 2004).

It is, therefore, intriguing to speculate that the physiological role of *PIN1* and related proteins that are said to act in auxin export to the neighboring cell for reimport (Blilou et al., 2005) is rather the efficient expulsion of this signaling molecule from the symplast to avoid auxin action in the wrong cells. In this case, the apical-to-basal auxin flow would occur mainly or exclusively in the apoplast, and the cell specificity of auxin action could be mediated by the cell-specific expression of auxin importer genes, e.g. in the hypophysis (e.g. *PIN4*; Friml et al., 2002; Weijers and Jürgens, 2005).

MATERIALS AND METHODS

Arabidopsis Lines Expressing *GFP* or Different *GFP* Fusions

Some of the Arabidopsis (*Arabidopsis thaliana*) lines used for the analyses presented were described before (*AtSUC2* promoter/*GFP* plants [Imlau et al., 1999]; *AtSUC3* promoter/*GFP* plants and *AtSUC3* promoter/*tmGFP9* plants [Meyer et al., 2004]). These and all other plants were grown under long-day conditions (16-h light/8-h dark) at 21°C. The *Escherichia coli* strain DH5α (Hanahan, 1983) was used for all cloning steps. Transformation of Arabidopsis was performed using *Agrobacterium tumefaciens* strain GV3101 (Holsters et al., 1980).

Construction of Plants Expressing *GFP* or *tmGFP9* under the Control of Arabidopsis *AtGL2* or *AtTT12* Promoters

For the construction of the *AtTT12* promoter/*GFP* construct, a 2,280-bp *TT12* promoter fragment was amplified from genomic DNA (ecotype Wassilewskija) by PCR using the primers TT12g-2262F (5′-GCA TGC CTG CAG GCA CTT GGC AAG ATT ATG TTC TGG TCA CC-3′) and TT12g+16R

(5′-CTC TGT GGA GCC CAT GGT CCG TTT ATT AGT TCC-3′). The fragment was cloned into pGEM-T Easy (Promega GmbH), sequenced, used to replace the *AtSUC2* promoter in front of the *GFP* ORF in pAF12 with *Hin*dIII and *Nco*I (Stadler et al., 2005), yielding pMH11, and finally cloned into the plant transformation vector pAF16 with *Hin*dIII and *Sac*I (Stadler et al., 2005), yielding pMH11a. pAF16 represents a modified version of the plant transformation vector pGPTV-bar (Becker et al., 1992). For the construction of the *AtTT12* promoter/*tmGFP9* construct, a genomic *AtSTP9* fragment was excised from pMH4 (Stadler et al., 2005) with *Nco*I and cloned into the unique *Nco*I site in the start ATG of *GFP* in pMH11. The resulting *AtTT12* promoter/*tmGFP9* box was cloned into pAF16 (with *Sda*I and *Xba*I) yielding pMH11c. The genomic *AtSTP9* fragment used in this construct contains two introns and codes for the 232 N-terminal amino acids (Schneidereit et al., 2003).

For the construction of the *AtGL2* promoter/*GFP* construct, a 2,140-bp *AtGL2* promoter fragment was amplified from genomic DNA (ecotype Wassilewskija) by PCR using the primers GL2g-2190F (5′-CTA ACA ATT CCC TAG GCC GTA CGA CGA-3′) and GL2g+4R (5′-CCA TGG ACA TAC AAA TCC TGT CCC TAG CTA GCT TC-3′). The fragment was cloned into pGEM-T Easy, sequenced, and used to replace the *AtSUC2* promoter in front of the *GFP* ORF in pAF12 with *Hin*dIII and *Nco*I (yielding pMH9) and finally cloned with *Hin*dIII and *Sac*I into the plant transformation vector pAF16 (yielding pMH9a). For the construction of the *AtGL2* promoter/*tmGFP9*, the above-mentioned genomic *AtSTP9* fragment was cloned into the unique *Nco*I site in the start ATG of *GFP* in pMH9. The resulting *AtGL2* promoter/*tmGFP9* box was cloned into pAF16 (*Hin*dIII and *Sac*I) yielding pMH9c.

Phloem Loading of HPTS

Phloem loading with the water-soluble HPTS (Molecular Probes; 2.5 mM solution in water) was performed essentially as described by Gisel and coworkers (1999).

CLSM

Seeds and embryos were imaged using CLSM (Leica TCS SP II; Leica Microsystems). For cell wall staining, the plant material was incubated in 0.5% propidium iodide for 10 min at room temperature and washed twice with water. GFP was excited by 488-nm light produced by an argon laser and observed using a detection window from 497 to 526 nm. Propidium iodide-stained cell walls were detected with the argon laser 488-nm line and a detection window of 595 to 640 nm.

For some analyses, we compared seeds from siliques of different developmental stages. The siliques were counted beginning at the top of the inflorescence. Silique number 1 represents the ovary of the first bud, where the white petals were visible (developmental stages were named as in Bowman, 1993).

Optical sections of picture stacks were made with the Leica confocal software 2.5 (Leica Microsystems) or with the Amira 3D visualization software 3.1 (Indeed Visual Concepts).

GFP fluorescence was quantified using the Analysis Docu 3.2 software package (Soft Imaging System).

ACKNOWLEDGMENT

We thank Marina Henneberg for excellent technical assistance.

Received May 18, 2005; revised June 23, 2005; accepted July 20, 2005; published September 16, 2005.

LITERATURE CITED

Becker D, Kemper E, Schell J, Mastersen R (1992) New plant binary vectors with selectable markers located proximal to the left T-DNA border. Plant Mol Biol **20:** 1195–1197

Berleth T, Jürgens G (1993) The role of the *MONOPTEROS* gene in organizing the basal body region of the *Arabidopsis* embryo. Development **118:** 575–587

Blilou I, Xu J, Wildwater M, Willemsen V, Paponov I, Friml J, Heidstra R, Aida M, Palme K, Scheres B (2005) The PIN auxin efflux facilitator network controls growth and patterning in *Arabidopsis* roots. Nature **433:** 39–44

Bowman JL (1993) Embryogenesis. *In* JL Bowman, ed, Arabidopsis: An Atlas of Morphology and Development. Springer-Verlag, New York, pp 351–401

Debeaujon I, Peeters AJM, Léon-Kloosterziel KM, Koornneef M (2001) The *TRANSPARENT TESTA12* gene of Arabidopsis encodes a multidrug secondary transporter-like protein required for flavonoid sequestration in vacuoles of the seed coat endothelium. Plant Cell **13:** 853–872

Fisher DB, Cash-Clark CE (2000a) Sieve tube unloading and post-phloem transport of fluorescent tracers and proteins injected into sieve tubes via severed aphid stylets. Plant Physiol **123:** 125–137

Fisher DB, Cash-Clark CE (2000b) Gradients in water potential and turgor pressure along the translocation pathway during grain filling in normal watered and water-stressed wheat plants. Plant Physiol **123:** 139–147

Fisher DB, Oparka K (1996) Post-phloem transport: principles and problems. J Exp Bot **47:** 1141–1154

Friml J, Benkova E, Blilou I, Wisniewska J, Hamann T, Ljung K, Woody S, Sandberg G, Scheres B, Jürgens G, et al (2002) AtPIN4 mediates sink-driven auxin gradients and root patterning in *Arabidopsis.* Cell **108:** 661–673

Friml J, Yang X, Michniewicz M, Weijers D, Quint A, Tietz O, Benjamins R, Ouwerkerk PBF, Ljung K, Sandberg G, et al (2004) A PINOID-dependent binary switch in apical-basal PIN polar targeting directs auxin efflux. Science **306:** 862–865

Gisel A, Barella S, Hempel FD, Zambryski PC (1999) Temporal and spatial regulation of symplastic trafficking during development in *Arabidopsis thaliana* apices. Development **126:** 1879–1889

Gottwald JR, Krysan PJ, Young JC, Evert RF, Sussman MR (2000) Genetic evidence for the in planta role of phloem-specific plasma membrane sucrose transporters. Proc Natl Acad Sci USA **97:** 13979–13984

Hamann T, Mayer U, Jürgens G (1999) The auxin-insensitive *bodenlos* mutation affects primary root formation and apical-basal patterning in the *Arabidopsis* embryo. Development **126:** 1387–1395

Hanahan D (1983) Studies on transformation of *E. coli* with plasmids. J Mol Biol **166:** 557–580

Haritatos E, Medville R, Turgeon R (2000) Minor vein structure and sugar transport in *Arabidopsis thaliana.* Planta **211:** 105–111

Holsters M, Silva B, Van Vliet F, Genetello C, De Block M, Dhaese P, Depicker A, Inze D, Engler G, Villarroel R, et al (1980) The functional organization of the nopaline *Agrobacterium tumefaciens* plasmid pTiC58. Plasmid **3:** 212–230

Hoth S, Schneidereit A, Lauterbach L, Scholz-Starke J, Sauer N (2005) Nematode infection triggers the de novo formation of unloading phloem that allows macromolecular trafficking of GFP into syncytia. Plant Physiol **138:** 383–392

Imlau A, Truernit E, Sauer N (1999) Cell-to-cell and long-distance trafficking of the green fluorescent protein in the phloem and symplastic unloading of the protein into sink tissues. Plant Cell **11:** 309–322

Jorgensen KE, Møller JV (1979) Use of flexible polymers as probes of glomerular pore size. Am J Physiol **236:** F103–F111

Kim I, Cho E, Crawford K, Hempel FD, Zambryski PC (2005) Cell-to-cell movement of GFP during embryogenesis and early seedling development in *Arabidopsis.* Proc Natl Acad Sci USA **102:** 2227–2231

Koroleva OA, Davies A, Deeken R, Thorpe MR, Tomos AD, Hedrich R (2000) Identification of a new glucosinolate-rich cell type in Arabidopsis flower stalk. Plant Physiol **124:** 599–608

Krishnan S, Dayanandan P (2003) Structural and histochemical studies on grain-filling in the caryopsis of rice (*Oryza sativa* L.). J Biosci **28:** 455–469

Le Maire M, Aggerbeck LP, Monteilhet C, Andersen JP, Møller JV (1986) The use of high-performance liquid chromatography for the determination of size and molecular weight of proteins: a caution and a list of membrane proteins suitable as standards. Anal Biochem **154:** 525–535

Lucas WJ, Bouché-Pillon S, Jackson DP, Nguyen L, Baker L, Ding B, Hake S (1995) Selective trafficking of KNOTTED1 homeodomain protein and its mRNA through plasmodesmata. Science **270:** 1980–1983

Mansfield SG, Bowman JL (1993) Ovules. *In* JL Bowman, ed, Arabidopsis: An Atlas of Morphology and Development. Springer-Verlag, New York, pp 299–331

Masucci JD, Rerie WG, Foreman DR, Zhang M, Galway ME, Marks MD, Schiefelbein JW (1996) The homeobox gene *GLABRA 2* is required for position-dependent cell differentiation in the root epidermis of *Arabidopsis thaliana.* Development **122:** 1253–1260

Meinke DW (1994) Seed development in Arabidopsis thaliana. *In* EM Meyerowitz and CR Somerville, eds, Arabidopsis. Cold Spring Harbor Laboratory Press, Cold Spring Harbor, NY, pp 253–295

Meyer S, Lauterbach C, Niedermeier M, Barth I, Sjolund RD, Sauer N (2004) Wounding enhances expression of *AtSUC3*, a sucrose transporter from Arabidopsis sieve elements and sink tissues. Plant Physiol **134:** 684–693

Meyer S, Truernit E, Hümmer C, Besenbeck R, Stadler R, Sauer N (2000) *AtSUC3*, a gene encoding a new *Arabidopsis* sucrose transporter, is expressed in cells adjacent to the vascular tissue and in a carpel cell layer. Plant J **24:** 869–882

Murray DR (1987) Nutritive role of seed coats in developing legume seeds. Am J Bot **74:** 1122–1137

Nakajima K, Sena G, Nawy T, Benfey PN (2001) Intercellular movement of the putative transcription factor SHR in root patterning. Nature **413:** 307–311

Offler E, Patrick JW (1984) Cellular structures, plasma membrane surface areas and plasmodesmatal frequencies of seed coats of *Phaseolus vulgaris* L. in relation to photosynthate transfer. Aust J Plant Physiol **11:** 79–99

Offler E, Patrick JW (1993) Pathway of photosynthate transfer in the developing seed of *Vicia faba* L. A structural assessment of the role of transfer cells in unloading from the seed coat. J Exp Bot **44:** 711–724

Oparka KJ, Gates PJ (1981) Transport of assimilates in the developing caryopsis of rice (*Oryza sativa* L.). Planta **152:** 388–396

Oparka KJ, Roberts AG, Boevink P, Santa Cruz S, Roberts I, Pradel KS, Imlau A, Kotlizky G, Sauer N, Epel B (1999) Simple, but not branched, plasmodesmata allow the nonspecific trafficking of proteins in developing tobacco leaves. Cell **97:** 743–754

Oparka KJ, Santa Cruz S (2000) The great escape: phloem transport and unloading of macromolecules. Annu Rev Plant Physiol Plant Mol Biol **51:** 323–347

Otegui M, Staehelin LA (2000) Syncytial-type cell plates: a novel kind of cell plate involved in endosperm cellularization of Arabidopsis. Plant Cell **12:** 933–947

Patrick JW (1997) Phloem unloading: sieve element unloading and post-sieve-element transport. Annu Rev Plant Physiol Plant Mol Biol **48:** 191–222

Patrick JW, Offler CE (1995) Post-sieve element transport of sucrose in developing seed. Aust J Plant Physiol **22:** 681–702

Patrick JW, Offler CE (2001) Compartmentation of transport and transfer events in developing seeds. J Exp Bot **52:** 551–564

Patrick JW, Offler CE, Wang X-D (1995) Cellular pathway of photosynthate transport in coats of developing seed of *Vicia faba* L. and *Phaseolus vulgaris* L. 1. Extent of transport through the coat symplast. J Exp Bot **46:** 35–47

Ribbeck K, Görlich D (2001) Kinetic analysis of translocation through nuclear pore complexes. EMBO J **20:** 1320–1330

Robinson-Beers K, Pruitt RE, Gasser CS (1992) Ovule development in wild-type Arabidopsis and two female-sterile mutants. Plant Cell **4:** 1237–1249

Ruiz-Medrano R, Xoconostle-Cazares B, Lucas WJ (1999) Phloem long-distance transport of CmNACP mRNA: implications for supracellular regulation in plants. Development **126:** 4405–4419

Sauer N, Stolz J (1994) SUC1 and SUC2: two sucrose transporters from *Arabidopsis thaliana*; expression and characterization in baker's yeast and identification of the histidine tagged protein. Plant J **6:** 67–77

Schneidereit A, Scholz-Starke J, Büttner M (2003) Functional characterization and expression analysis of the glucose-specific AtSTP9 monosaccharide transporter in pollen of Arabidopsis. Plant Physiol **133:** 1–9

Sessions A, Yanofsky MF, Weigel D (2000) Cell-cell signaling and movement by the floral transcription factors LEAFY and APETALA1. Science **289:** 779–782

Stadler R, Sauer N (1996) The *Arabidopsis thaliana AtSUC2* gene is specifically expressed in companion cells. Bot Acta **109:** 299–306

Stadler R, Wright KM, Lauterbach C, Amon G, Gahrtz M, Feuerstein A, Oparka KJ, Sauer N (2005) Expression of *GFP*-fusions in *Arabidopsis* companion cells reveals non-specific protein trafficking into sieve elements and identifies a novel post-phloem domain in roots. Plant J **41:** 319–331

Sun K, Hunt K, Hauser BA (2004) Ovule abortion in Arabidopsis is triggered by stress. Plant Physiol **135:** 2358–2367

Szymanski DB, Jilk RA, Pollock SM, Marks MD (1998) Control of *GL2* expression in *Arabidopsis* leaves and trichomes. Development **125:** 1161–1171

Tegeder M, Wang X-D, Frommer WB, Offler CE, Patrick JW (1999) Sucrose transport into developing seeds of *Pisum sativum* L. Plant J **18:** 151–161

Terry BR, Matthews EK, Haseloff J (1995) Molecular characterization of recombinant green fluorescent protein by fluorescence correlation microscopy. Biochem Biophys Res Commun **217:** 21–27

Truernit E, Sauer N (1995) The promoter of the *Arabidopsis thaliana* SUC2 sucrose-H^+ symporter gene directs expression of beta-glucuronidase to the phloem: evidence for phloem loading and unloading by SUC2. Planta **196:** 564–570

Wang N, Fisher DB (1994) The use of fluorescent tracers to characterize the post-phloem transport pathway in maternal tissue of developing wheat grains. Plant Physiol **104:** 17–27

Wang N, Offler CE, Patrick JW (1995) The cellular pathway of photosynthate transfer in the developing wheat grain. II. A structural analysis and histochemical studies of the pathway from the crease phloem to the endosperm cavity. Plant Cell Environ **18:** 373–388

Wang N, Offler CE, Patrick JW, Ugalde TD (1994) The cellular pathway of photosynthate transfer in the developing wheat grain. I. Delineation of a potential transfer pathway using fluorescent dyes. Plant Cell Environ **17:** 257–266

Weber H, Borisjuk L, Heim U, Buchner P, Wobus U (1997a) Seed coat-associated invertases of fava bean control both unloading and storage functions: cloning of cDNAs and cell type-specific expression. Plant Cell **7:** 1835–1846

Weber H, Borisjuk L, Wobus U (1997b) Sugar import and metabolism during seed development. Trends Plant Sci **2:** 169–174

Weijers D, Jürgens G (2005) Auxin and embryo axis formation: the ends in sight? Curr Opin Plant Biol **8:** 32–37

Weise A, Barker L, Kühn C, Lalonde S, Buschmann H, Frommer WB, Ward JM (2000) A new subfamily of sucrose transporters, SUT4, with low affinity/high capacity is localized in enucleate sieve elements of plants. Plant Cell **12:** 1345–1356

Windsor JB, Symonds VV, Mendenhall J, Lloyd AM (2000) *Arabidopsis* seed coat development: morphological differentiation of the outer integument. Plant J **22:** 483–493

Wright K, Oparka KJ (1996) The fluorescent probe HPTS as a phloem-mobile, symplastic tracer: an evaluation using confocal laser scanning microscopy. J Exp Bot **47:** 439–445

Wu X, Dinneny JR, Crawford KM, Rhee Y, Citovsky V, Zambryski PC, Weigel D (2003) Modes of intercellular transcription factor movement in the *Arabidopsis* apex. Development **130:** 3735–3745

Xoconostle-Cazares B, Xiang Y, Ruiz-Medrano R, Wang HL, Monzer J, Yoo BC, McFarland KC, Franceschi VR, Lucas WJ (1999) Plant paralog to viral movement protein that potentiates transport of mRNA into the phloem. Science **283:** 94–98

Yeung EC (1980) Embryogeny of *Phaseolus*: the role of the suspensor. Z Pflanzenphysiol **96:** 17–28

Yeung EC, Meinke DW (1993) Embryogenesis in angiosperms: development of the suspensor. Plant Cell **5:** 1371–1381

Zhang LY, Peng YB, Pelleschi-Travier S, Fan Y, Lu YF, Lu YM, Gao XP, Shen YY, Delrot S, Zhang DP (2004) Evidence for apoplasmic phloem unloading in developing apple fruit. Plant Physiol **135:** 574–586